Hole Delocalization in Oxidized Cerium(IV) Porphyrin Sandwich Complexes

Robert J. Donohoe, John K. Duchowski, and David F. Bocian*

Contribution from the Department of Chemistry, Carnegie Mellon University, Pittsburgh, Pennsylvania 15213. Received December 18, 1987

Abstract: Optical absorption, electron paramagnetic resonance, and resonance Raman spectra are reported for the one-electron oxidation products of the Ce(IV) sandwich porphyrins, Ce(OEP)$_2$ and Ce(TPP)$_2$ (OEP = octaethylporphyrin; TPP = tetraphenylporphyrin). These data, in conjunction with electrochemical measurements, indicate that the holes of both oxidized species are delocalized on the vibrational and probably the electronic time scales. In Ce(OEP)$_2^+$, the hole is delocalized through purely porphyrin–porphyrin interactions. In Ce(TPP)$_2^+$, delocalization is further facilitated by participation of the f orbitals of the Ce(IV) ion. The different characteristics of the redox orbitals of Ce(OEP)$_2^+$ and Ce(TPP)$_2^+$ are accounted for by the fact that oxidation occurs from an a_{1u}-like orbital in the former complex and from an a_{2u}-like orbital in the latter.

I. Introduction

Electronic interactions between porphyrinic π systems in close proximity play a pivotal role in such diverse systems as photosynthetic proteins[1] and organic conductors.[2] The bacterial photosynthetic reaction center is comprised in part of two of the bacteriochlorophyll molecules which are closely associated and constitute the special pair.[3-5] This supermolecule serves as the primary electron donor in light-energy conversion.[1] Strong electronic interactions between molecules within synthetic stacked or bridged aggregates of metalloporphyrins and metallophthalocyanines impart unique properties to these systems. In particular, such aggregates exhibit large electrical conductivities which suggest that these materials may be of use in the development of the next generation of electronic devices.[2,6-12] The facile electron transfer which occurs in these natural and synthetic π-system aggregates has spurred a renewed interest in the detailed characterization of their electronic structure.[10,13]

Before a thorough understanding of complex aggregates can be achieved, it is first necessary to delineate the electronic properties of the simplest multimer, namely a dimer. Numerous examples of porphyrinic dimers are known and include π complexes,[14,15] covalently linked species,[16-19] metal–metal bonded

systems,[20-22] and single and multiple atom bridged complexes.[12,23-37] Of these many forms, the lanthanide sandwich com-

(1) Okamura, M. Y.; Feher, G.; Nelson, N. In *Photosynthesis: Energy Conversion by Plants and Bacteria*; Academic Press: New York, 1982; Vol. 1, pp 195–272.

(2) Hoffman, B. M.; Ibers, J. A. *Acc. Chem. Res.* **1983**, *16*, 15–21, and references therein.

(3) Diesenhofer, J.; Epp, O.; Miki, K.; Huber, R.; Michel, H. *J. Mol. Biol.* **1984**, *180*, 385–398.

(4) Diesenhofer, J.; Epp, O.; Miki, K.; Huber, R.; Michel, H. *Nature (London)* **1985**, *318*, 618–624.

(5) Chang, C.-H.; Tiede, D.; Tang, J.; Smith, U.; Norris, J.; Shiffer, M. *FEBS Lett.* **1986**, *205*, 82–86.

(6) (a) Martinsen, J.; Stanton, J. L.; Greene, R. L.; Tanaka, J.; Hoffman, B. M.; Ibers, J. A. *J. Am. Chem. Soc.* **1985**, *107*, 6915–6920. (b) Ogawa, M. Y.; Martinsen, J.; Palmer, S. M.; Stanton, J. L.; Tanaka, J.; Greene, R. L.; Hoffman, B. M.; Ibers, J. A. *Ibid.* **1987**, *109*, 1115–1121.

(7) Turek, P.; Petit, P.; André, J.-J.; Simon, J.; Even, R.; Boudjema, B.; Guillaud, G.; Maitrot, M. *J. Am. Chem. Soc.* **1987**, *109*, 5119–5122.

(8) Nohr, R. S.; Kuznesof, P. M.; Wynne, K. J.; Kenney, M. E.; Siebenman, P. G. *J. Am. Chem. Soc.* **1981**, *103*, 4371–4377.

(9) Diel, B. N.; Inabe, T.; Lyding, J. W.; Schoch, K. F., Jr.; Kannewurf, C. R.; Marks, T. J. *J. Am. Chem. Soc.* **1983**, *105*, 1551–1567.

(10) Pietro, W. J.; Marks, T. J.; Ratner, M. A. *J. Am. Chem. Soc.* **1985**, *107*, 5387–5391.

(11) Diel, B. N.; Inabe, T.; Taggi, N. K.; Lyding, J. W.; Schneider, O.; Hanack, M.; Kannewurf, C. R.; Marks, T. J.; Schwartz, L. H. *J. Am. Chem. Soc.* **1984**, *106*, 3207–3214.

(12) Collman, J. P.; McDevitt, J. T.; Leidner, C. R.; Yee, G. T.; Torrance, J. B.; Little, W. A. *J. Am. Chem. Soc.* **1987**, *109*, 4606–4614.

(13) Hale, P. D.; Pietro, W. J.; Ratner, M. A.; Ellis, D. E.; Marks, T. J. *J. Am. Chem. Soc.* **1987**, *109*, 5943–5947.

(14) Svec, W. A. In *The Porphyrins*; Dolphin, D., Ed.; Academic Press: New York, 1978; Vol. V, pp 341–399.

(15) (a) Shelnutt, J. A.; Dobry, M. M.; Satterlee, J. D. *J. Phys. Chem.* **1984**, *88*, 4980–4987. (b) Shelnutt, J. A. *Ibid.* **1984**, *88*, 4988–4992.

(16) Wasielewski, M. R.; Svec, W. A.; Cope, B. T. *J. Am. Chem. Soc.* **1978**, *100*, 1961–1962.

(17) Boxer, S. G.; Closs, G. L. *J. Am. Chem. Soc.* **1976**, *98*, 5406–5408.

(18) Bucks, R. R.; Boxer, S. G. *J. Am. Chem. Soc.* **1982**, *104*, 340–343.

(19) (a) Collman, J. P.; Denisevich, P.; Konai, Y.; Marrocco, M.; Koval, C.; Anson, F. C. *J. Am. Chem. Soc.* **1980**, *102*, 6027–6036. (b) Collman, J. P.; Anson, F. C.; Barnes, C. E.; Bencosme, C. S.; Geiger, T.; Evitt, E. R.; Kreh, R. P.; Meier, K.; Pettman, R. B. *Ibid.* **1983**, *105*, 2644–2699. (c) Collman, J. P.; Bencosme, C. S.; Durand, R. R., Jr.; Kreh, R. P.; Anson, F. C. *Ibid.* **1983**, *105*, 2699–2703. (d) Collman, J. P.; Bencosme, C. S.; Barnes, C. E.; Miller, B. D. *Ibid.* **1983**, *105*, 2704–2710.

(20) (a) Collman, J. P.; Barnes, C. E.; Collins, T. J.; Brothers, P. J.; Gallucci, J.; Ibers, J. A. *J. Am. Chem. Soc.* **1981**, *103*, 7030–7032. (b) Collman, J. P.; Barnes, C. E.; Woo, L. K. *Proc. Natl. Acad. Sci. U.S.A.* **1983**, *80*, 7684–7688. (c) Collman, J. P.; Barnes, C. E.; Brothers, P. J.; Collins, T. J.; Ozawa, T.; Gallucci, J. C.; Ibers, J. A. *J. Am. Chem. Soc.* **1984**, *106*, 5151–5163. (d) Collman, J. P.; Barnes, C. E.; Swepston, P. N.; Ibers, J. A. *Ibid.* **1984**, *106*, 3500–3510. (e) Collman, J. P.; Woo, L. K. *Proc. Natl. Acad. Sci. U.S.A.* **1984**, *81*, 2592–2596.

(21) Ogoshi, H.; Setsune, J.; Hoshida, Z. *J. Am. Chem. Soc.* **1977**, *99*, 3869–3870.

(22) Wayland, B. B.; Newman, A. *Inorg. Chem.* **1981**, *20*, 3093–3097.

(23) Tsutsui, M.; Taylor, G. A. In *Porphyrins and Metalloporphyrins*; Smith, K. M., Ed.; Elsevier: Amsterdam, 1975; pp 279–313.

(24) Fleischer, E. B.; Srivastava, T. S. *J. Am. Chem. Soc.* **1969**, *91*, 2403–2405.

(25) Summerville, D. A.; Cohen, I. A. *J. Am. Chem. Soc.* **1976**, *98*, 1747–1752.

(26) Mansuy, D.; Lecomte, J.-P.; Chottard, J.-C.; Bartoli, J.-F. *Inorg. Chem.* **1981**, *20*, 3119–3121.

(27) Wynne, K. J.; Nohr, R. S. *Mol. Cryst. Liq. Cryst.* **1981**, *81*, 243–254.

(28) Dirk, C. W.; Inabe, T.; Schoch, K. F., Jr.; Marjs, T. J. *J. Am. Chem. Soc.* **1983**, *105*, 1539–1550.

(29) Ercolani, C.; Gardini, M.; Monacelli, F.; Pennesi, G.; Rossi, G. *Inorg. Chem.* **1983**, *22*, 2584–2589.

(30) (a) Schneider, O.; Hanack, M. *Mol. Cryst. Liq. Cryst.* **1982**, *81*, 273–284. (b) Hanack, M. *Ibid.* **1984**, *105*, 133–149.

(31) (a) Buchler, J. W.; Kapellmann, H.-G.; Knoff, M.; Lay, K.-L.; Pfeifer, S. *Z. Naturforsch., B: Anorg. Chem., Org. Chem.* **1983**, *38B*, 1339–1345. (b) Buchler, J. W.; Knoff, M. In *Optical Properties and Structure of Tetrapyrroles*; Blauer, G., Sund, H., Eds.; de Gruyter: West Berlin, 1985; pp 91–105. (c) Buchler, J. W.; Elsässer, K.; Kihn-Botulinski, M.; Scharbert, B. *Angew. Chem., Int. Ed. Engl.* **1986**, *25*, 286–287. (d) Buchler, J. W.; DeCian, A.; Fischer, J.; Kihn-Botulinski, M.; Paulus, H.; Weiss, R. *J. Am. Chem. Soc.* **1986**, *108*, 3652–3659. (e) Buchler, J. W.; de Cian, A.; Fischer, J.; Kihn-Botulinski, M.; Weiss, R. *Inorg. Chem.* **1988**, *27*, 339–345. (f) Buchler, J. W.; Scharbert, B. *J. Am. Chem. Soc.* **1988**, *110*, 4272–4276.

(32) Girolami, G. S.; Milam, S. N.; Suslick, K. S. *Inorg. Chem.* **1987**, *26*, 343–344.

(33) Kasuga, K.; Tsutsui, M. *Coord. Chem. Rev.* **1980**, *32*, 67–95.

(34) Kasuga, K.; Tsutsui, M.; Petterson, R. C.; Tatsumi, K.; Van Opdenbosch, N.; Pepe, G.; Meyer, E. F., Jr. *J. Am. Chem. Soc.* **1980**, *102*, 4835–4836.

(35) Lux, F.; Dempf, D.; Graw, D. *Angew. Chem., Int. Ed. Engl.* **1968**, *7*, 819–820.

plexes are of particular interest due to the especially close proximity of their π systems.[31,33,34,38] Sandwich complexes of Ce(IV) with OEP (OEP = octaethylporphyrin) and TPP (TPP = tetraphenylporphyrin) have been prepared by Buchler and co-workers.[31] Crystallographic studies of Ce(OEP)$_2$ show that the core atoms of the two π macrocycles are on average separated by 3.4 Å, while the distance between the planes defined by the pyrrole nitrogen atoms is only 2.7 Å.[31d] The Soret maxima of both Ce(OEP)$_2$ and Ce(TPP)$_2$ are significantly shifted to the blue of those of monomeric lanthanide porphyrins. This blue shift has been attributed to excitonic interactions between the B-excited states of the two porphyrin macrocycles.[31b] In addition, electrochemical generation of the Ce(OEP)$_2^+$ π cation radical occurs at a potential considerably more cathodic than is observed for any monomeric OEP π cation radical.[31c] This ease of oxidation suggests that the redox orbital is, to some extent, delocalized over both porphyrin π systems. The presence of near IR absorption features attributed to intervalence charge-transfer transitions provides further evidence for π system interaction in the Ce(OEP)$_2^+$ and Ce(TPP)$_2^+$ complexes.[31f]

In this paper, we examine the electrochemical properties and the UV–vis, electron paramagnetic resonance (EPR) and resonance Raman (RR) spectra of Ce(OEP)$_2^+$ and Ce(TPP)$_2^+$. For comparative purposes, the spectra of the monomeric lanthanide porphyrin π cation radicals (LuOEPOH)$^+$ and (LuTPPOH)$^+$ have also been acquired. Collectively, these data provide insight into the extent of redox orbital delocalization in the Ce(IV) porphyrin sandwich π cation radicals.

II. Experimental Section

LuOEPOH and LuTPPOH were synthesized by the imidazole melt method described by Srivastava[39] and purified by column chromatography on MgCO$_3$. Ce(OEP)$_2$ was the generous gift of Professor D. Holten of Washington University. Ce(TPP)$_2$ was synthesized by following the general procedure prescribed by Buchler and co-workers.[31a] However, the reaction was found to proceed very slowly; therefore, the reflux of H$_2$TPP (Midcentury) with Ce^{III}(acetylacetonate)$_3$·4H$_2$O (Strem Chemicals) in 1,2,4-trichlorobenzene (Alfa, 99+%) was allowed to proceed for 3 days. Even after this period, the reaction was found to be largely incomplete. The appearance of a shoulder on the blue side of the free base Soret absorption band was the only discernible indication of the formation of Ce(TPP)$_2$. After removal of the solvent by vacuum distillation, the residue was repeatedly washed with warm toluene to remove the bulk of the unreacted H$_2$TPP, and the remaining solid was chromatographed on a Sephadex LH-20 column (2.5 × 40 cm) in CH$_2$Cl$_2$. Only the initial fraction of the band was collected.

The oxidized complexes were prepared in a Vacuum Atmospheres Model HE-43 glovebox equipped with a Model 493 Dri-Train by using electrochemical instrumentation which has been described elsewhere.[40] The integrity of the oxidized products was confirmed by cyclic voltammetry and coulometry. The samples were prepared in CH$_2$Cl$_2$ which was purified by vacuum distillation off of P$_2$O$_5$. Tetrabutylammonium perchlorate, TBAP (Kodak, recrystallized twice from absolute ethanol), served as the supporting electrolyte. The oxidized samples were typically ~1 mM complex and 0.1 M TBAP except for Ce(TPP)$_2^+$ which was prepared at 0.2 mM due to low solubility of the neutral complex. Attempts to isolate the oxidized products in solid form by solvent evaporation of bulk electrolyzed solutions resulted in partial reconversion to the neutral species except for Ce(OEP)$_2^+$. As was originally reported by Buchler and co-workers,[31c] this latter complex is quite stable under dry atmospheres and can be readily obtained as the solid salt. We isolated Ce(OEP)$^+$ from the supporting electrolyte by column chromatography on oven-dried LH-20 in CH$_2$Cl$_2$.

UV–vis samples of the neutral and oxidized products of a given complex were aliquoted from a single solution before and after oxidation. The Soret region extinction coefficients were determined from diluted samples. EPR samples were aliquoted directly from the electrochemical cell into quartz tubes equipped with ground glass joints which were subse-

(36) Gieren, A.; Hoppe, W. *J. Chem. Soc., Chem. Commun.* 1971, 413–414.
(37) Kirin, I. S.; Kolyadin, A. B.; Lychev, A. A. *J. Struct. Chem. (Engl. Transl.)* 1974, *15*, 415–418.
(38) Yan, X.; Holten, D. *J. Phys. Chem.* 1988, *92*, 409–413.
(39) Srivastava, T. S. *Bioinorg. Chem.* 1978, *8*, 61–76.
(40) Donohoe, R. J.; Atamian, M.; Bocian, D. F. *J. Am. Chem. Soc.* 1987, *109*, 5593–5599.

Table I. Half-Wave Potentials $(E_{1/2})^a$ for the Complexes

| complex | redox couple($E_{1/2}$) | | | |
	$E_{1/2}^{+2/+1}$	$E_{1/2}^{+1/0}$	$E_{1/2}^{0/-1}$	$E_{1/2}^{-1/-2}$
Ce(OEP)$_2$	+0.58	+0.26	-0.51^b	-1.77^c
LuOEPOH	d	+0.69	-1.68^b	
Ce(TPP)$_2$	+1.19	+0.79	-0.16	-1.73^c
LuTPPOH	d	+0.86	-1.26	

^{a} Potentials listed are V versus Ag/AgCl (saturated KCl). ^{b} This wave is quite irreversible. ^{c} This potential is from the peak of the cathodic portion of an irreversible wave. ^{d} Scanning through this irreversible wave results in sample decomposition.
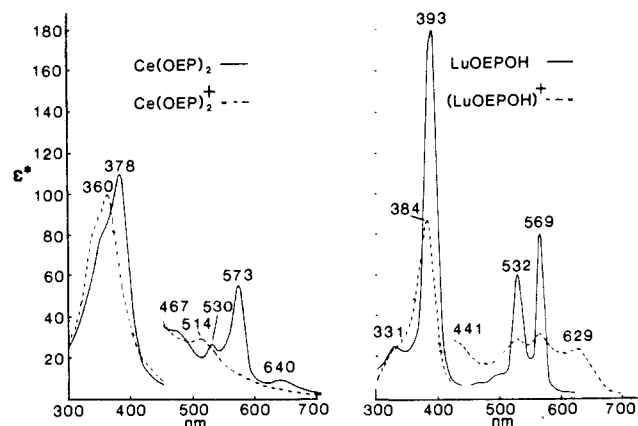

Figure 1. Absorption spectra of the neutral (—) and singly oxidized (---) Ce(OEP)$_2$ (left) and LuOEPOH (right) complexes in CH$_2$Cl$_2$ (* × 10^{-3} 1 mol^{-1} cm^{-1}).

quently sealed and transferred into the cavity of an IBM Instruments ER-300 X-band EPR spectrometer for data collection. Low-temperature EPR spectra were obtained by using a finger dewar (77 K) or an Oxford Instruments ESR-900 cryostat (4.2 K). RR solution samples were also transferred directly from the working solutions and sealed in capillary cells. RR solid samples were suspended in compressed pellets with a supporting medium of Na$_2$SO$_4$. The RR spectra were acquired by using instrumentation described elsewhere.[40] The incident laser powers were approximately 50 mW. The spectral slit width was 3 cm^{-1}.

III. Results

A. Electrochemistry. The redox potentials [V versus Ag/AgCl (saturated KCl)] for the monomeric Lu(III) and dimeric Ce(IV) OEP and TPP complexes are given in Table I. The first ring oxidation of Ce(OEP)$_2$ occurs at 0.26 V which is 0.43 V cathodic of the analogous oxidation of LuOEPOH. In contrast, oxidation of Ce(TPP)$_2$ occurs at 0.79 V which is only 0.07 V cathodic of that of LuTPPOH. These results suggest that the oxidation of Ce(TPP)$_2$ is influenced by metal orbital particpiation (vide infra). The first reductions of Ce(OEP)$_2$ and Ce(TPP)$_2$ occur at -0.51 and -0.16 V, respectively. These values are extremely anodic compared with the first (porphyrin-centered) reductions of LuOEPOH (-1.68 V) and LuTPPOH (-1.26 V) and indicate that the first reductions of the Ce(IV) complexes involve an orbital which is primarily metal in character.[41]

B. Absorption Spectra. The absorption spectra of Ce(OEP)$_2$ and Ce(OEP)$_2^+$ are compared with those of LuOEPOH and (LuOEPOH)$^+$ in Figure 1. The spectra for the analogous TPP complexes are shown in Figure 2. The Soret maxima of the cations of all four species are blue shifted relative to those of their neutral counterparts. The appearance of the absorption spectra of the cations does not readily aid in the assignment of the redox orbitals.[42] A particularly noteworthy aspect of the absorption spectra of the two Ce(IV) porphyrin cations is that they do not appear to be comprised of features associated with separate neutral and oxidized chromophores isolated within a single a molecule. Such composite absorption spectra have been observed in tran-

(41) Felton, R. H. In *The Porphyrins*; Dolphin, D., Ed.; Academic Press: New York, 1978; Vol. V, pp 53–125.
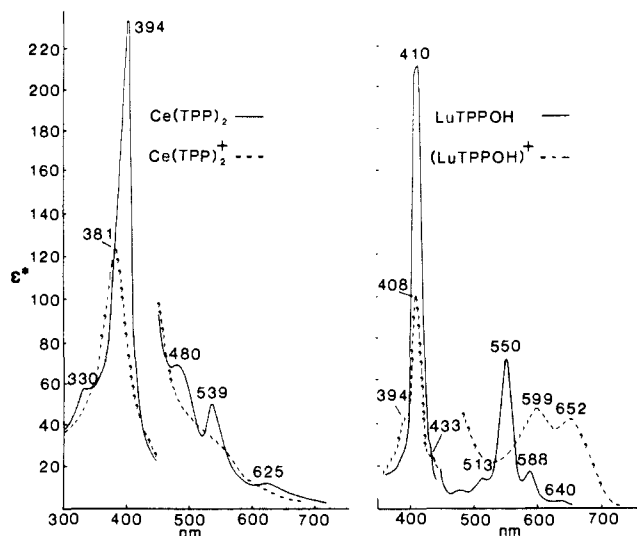(42) Edwards, W. D.; Zerner, M. C. *Can. J. Chem.* 1985, *63*, 1763–1772.

Figure 2. Absorption spectra of the neutral (—) and singly oxidized (---) Ce(TPP)$_2$ (left) and LuTPPOH (right) complexes in CH$_2$Cl$_2$ (* × 10^{-3} l mol^{-1} cm^{-1}).
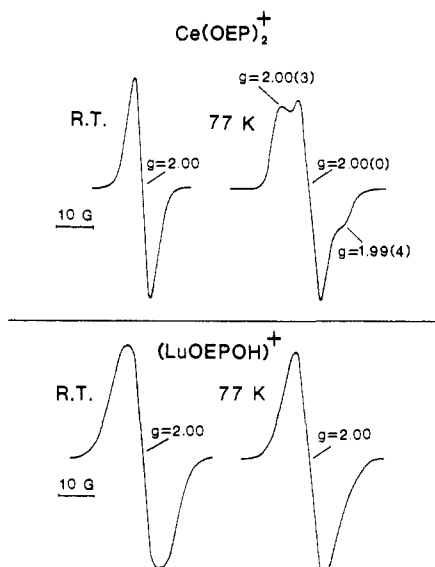

Figure 3. Electron paramagnetic resonance spectra of Ce(OEP)$_2^+$ (upper panel) and (LuOEPOH)$^+$ (lower panel) in CH$_2$Cl$_2$ at room temperature and 77 K.

Figure 4. Electron paramagnetic resonance spectra of Ce(TPP)$_2^+$ at 77 K (upper panel) and (LuTPPOH)$^+$ at room temperature and 77 K (lower panel). The solvent is CH$_2$Cl$_2$ for both complexes.

sition-metal complexes wherein the redox orbital is known to be localized on one ligand of a multiligand system.[43-45]

Absorption spectra were also obtained for Ce(OEP)$_2^-$ and Ce(TPP)$_2^-$ (not shown). The general appearance of the spectra of these anions is similar to that of the neutral complexes. No features are observed for the reduced species which would suggest that the redox orbital contains a large amount of porphyrin character.[41] These results are consistent with the electrochemical measurements which indicate that the first reduction involves an orbital that is primarily metal centered. Buchler and co-workers have reached a similar conclusion.[31f]
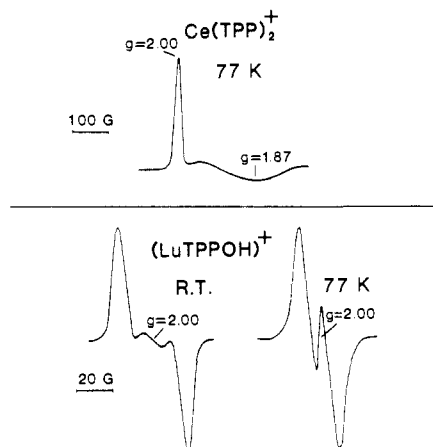
C. EPR Spectra. The EPR spectra of (LuOEPOH)$^+$ and (LuTPPOH)$^+$ are shown in the bottom panels of Figures 3 and 4, respectively. These spectra provide a clear distinction between the nature of the redox orbitals of the OEP and TPP systems. The EPR spectrum of (LuOEPOH)$^+$ is a simple first derivative signal centered at g = 2.00 with no resolved hyperfine structure at either room or low temperature. The general appearance of the EPR spectrum and, in particular, the lack of resolved hyperfine structure due to the I = 7/2 ^{175}Lu nucleus is indicative of a ^{2}A$_{1u}$ ground state.[46] A number of metallo OEP π cation radicals, including (CuOEP)$^+$, (MgOEP)$^+$, and (ZnOEP)$^+$, also exhibit ^{2}A$_{1u}$ ground states. In contrast to the signal observed for (LuOEPOH)$^+$, the EPR spectrum of (LuTPPOH)$^+$ displays hyperfine structure due to the I = 7/2 ^{175}Lu nucleus at both room and low temperature. [The room temperature EPR spectrum of (LuTPPOH)$^+$ displays a weak feature at g = 2.00 which is due to sample aggregation. This feature becomes more pronounced in the frozen solution spectrum.] The appearance of metal hyperfine structure is consistent with a ^{2}A$_{2u}$ ground state, which is typical of metallo TPP π cation radicals.[46] The general features observed in the room temperature EPR spectrum of (LuTPPOH)$^+$ are quite similar to those observed in the room temperature spectrum of (CoTPPX)$^+$ (I = 7/2 for ^{59}Co).[47] As is the case for (CoTPPX)$^+$, the EPR signal from (LuTPPOH)$^+$ is sufficiently broad that only the outer two lines of eight-line hyperfine pattern due to the metal ion are observed. Computer simulations of the EPR spectrum of (LuTPPOH)$^+$ yield ^{175}Lu and ^{14}N hyperfine coupling constants of 5.14 G (14.4 MHz) and 1.44 G (4.03 MHz), respectively (with a 1 G line width). In comparison, the ^{59}Co hyperfine coupling constant for the ^{2}A$_{2u}$ ground state of (CoTPPX)$^+$ is 5.7 G (16.0 MHz).[47]

The EPR spectra of Ce(OEP)$_2^+$ are displayed in the top panel of Figure 3. As is the case for (LuOEPOH)$^+$, the room temperature EPR spectrum of Ce(OEP)$_2^+$ is a simple first derivative signal centered at g = 2.00 with no resolved hyperfine structure (hyperfine structure can arise only from the porphyrin moieties because I = 0 for the principal cerium isotopes, ^{140}Ce and ^{142}Ce). The similarity of the spectra of the Lu(III) and Ce(IV) complexes indicates that the nature of the redox orbital is the same for the two systems. Reduction of the temperature to 77 K does not result in the resolution of any hyperfine structure for Ce(OEP)$^+$; however, the signal does become slightly anisotropic. Comparison of the room temperature signals of Ce(OEP)$_2^+$ and (LuOEPOH)$^+$ shows that the peak-to-peak line width of the former complex (~4 G) is approximately half that of the latter (~8 G). This reduced line width for the sandwich porphyrin cation compared with that of the monomeric cation could be the result of unresolved ^{175}Lu

(43) Heath, G. A.; Yellowlees, L. J.; Braterman, P. S. *J. Chem. Soc., Chem. Commun.* **1981**, 287–289.

(44) Elliot, C. M.; Hershenhart, E. *J. Am. Chem. Soc.* **1982**, *104*, 7519–7526.

(45) (a) Angle, S. M.; DeArmond, M. K.; Donohoe, R. J.; Wertz, D. W. *J. Phys. Chem.* **1985**, *89*, 282–285. (b) Donohoe, R. J.; Tait, C. D.; DeArmond, M. K.; Wertz, D. W. *Spectrochim. Acta* **1986**, *42A*, 233–240. (c) Tait, C. D.; MacQueen, D. B.; Donohoe, R. J.; DeArmond, M. K.; Hanck, K. W.; Wertz, D. W. *J. Phys. Chem.* **1986**, *90*, 1766–1771. (d) Donohoe, R. J.; Tait, C. D.; DeArmond, M. K.; Wertz, D. W. *Ibid.* **1986**, *90*, 3923–3926. (e) Donohoe, R. J.; Tait, C. D.; DeArmond, M. K.; Wertz, D. W. *Ibid.* **1986**, *90*, 3827–3930.

(46) Fajer, J.; Davis, M. S. In *The Porphyrins*; Dolphin, D., Ed.; Academic Press: New York, 1978; Vol. IV, pp 197–256, and references therein.

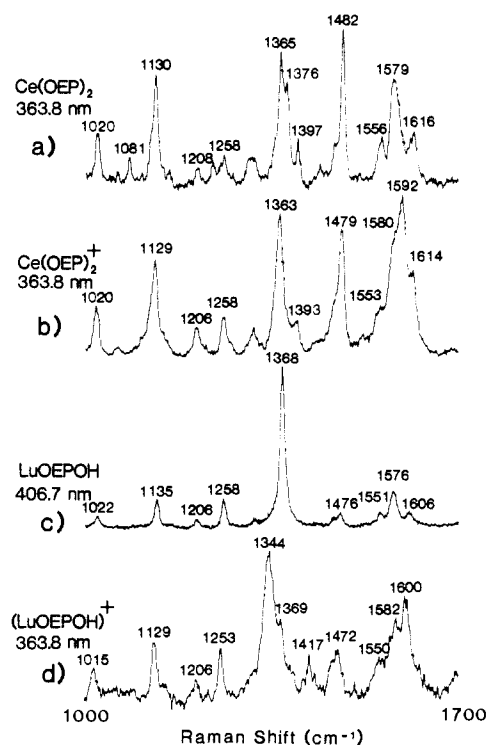(47) Wolberg, A.; Manassen, J. *J. Am. Chem. Soc.* **1970**, *92*, 2982–2991.

Figure 5. High-frequency portions of the Soret excitation resonance Raman spectra: (a), Ce(OEP)$_2$; (b), Ce(OEP)$_2^+$; (c), LuOEPOH; (d), (LuOEPOH)$^+$ obtained with the given excitation energies. The Ce(IV) complexes are solids in Na$_2$SO$_4$ pellets. The Lu(III) complexes are in CH$_2$Cl$_2$ solutions.

Figure 6. High-frequency portions of the Soret excitation resonance Raman spectra: (a), Ce(TPP)$_2$; (b), Ce(TPP)$_2^+$ obtained with the given excitation energy. Both complexes are in CH$_2$Cl$_2$ solutions. Solvent peaks are marked by the symbol #.

Table II. Resonance Raman Frequencies (cm^{-1}) for the Neutral and Oxidized OEP Complexes Examined in This Study

band[a]	Ce(OEP)$_2$	Ce-(OEP)$_2^+$	Δ	LuOE-POH	(LuOE-POH)$^+$	Δ
ν_4	1376	1363	−13	1368	1344	−24
ν_3	1482	1479	−3	1476	1472	−4
ν_{11}	1556	1580	+24	1551	1582	+31
ν_2	1579	1592	+13	1576	1600	+24

a Mode numbering and assignments follow ref 50 and 51.

hyperfine structure in the spectrum of the latter system. A more intriguing explanation for the reduced line width of the sandwich complex is that the hole is delocalized over both porphyrin rings on the EPR time scale. A similar reduction in line width is observed for cation radicals of dimeric versus monomeric chlorophyll species.[46,48] Because the frozen solution EPR spectrum of Ce(OEP)$_2^+$ is slightly anisotropic, it is not possible to determine from line width measurements whether the hole becomes localized at low temperatures. However, the RR data indicate that localization of the hole will not occur even at extremely low temperatures (vide infra).

The 77 K EPR spectrum of Ce(TPP)$_2^+$ is shown in the top panel of Figure 4. No EPR signal was detected for this complex at room temperature. Unlike the Ce(OEP)$_2^+$ complex, the spectrum for the TPP system is highly anisotropic. The EPR spectrum of Ce(TPP)$_2^+$ was also recorded at 4.2 K (not shown). This spectrum is identical with that obtained at 77 K both with respect to the degree of anisotropy and the line widths of the signals. The anisotropy is indicative of substantial metal character in the ground state of the oxidized complex. The lack of an EPR signal at room temperature is consistent with metal participation in the redox orbital. Unpaired electron density on the cerium metal center would be expected to give rise to rapid relaxation at room temperature. In this regard, lanthanide complexes typically do not exhibit EPR spectra above 20 K.[49]

D. RR Spectra. The Soret excitation RR spectra of the neutral and oxidized Ce(OEP)$_2$ complexes are shown in Figure 5 (parts a and b, respectively). The analogous RR spectra of the Ce(TPP)$_2$ complexes are shown in Figure 6 (parts a and b). The Soret excitation RR spectra of the neutral and oxidized LuOEPOH complexes are shown in Figure 5 (parts c and d). RR spectra of (LuTPPOH)$^+$ could not be obtained owing to extremely facile photoreduction of both solid and solution samples. RR spectra
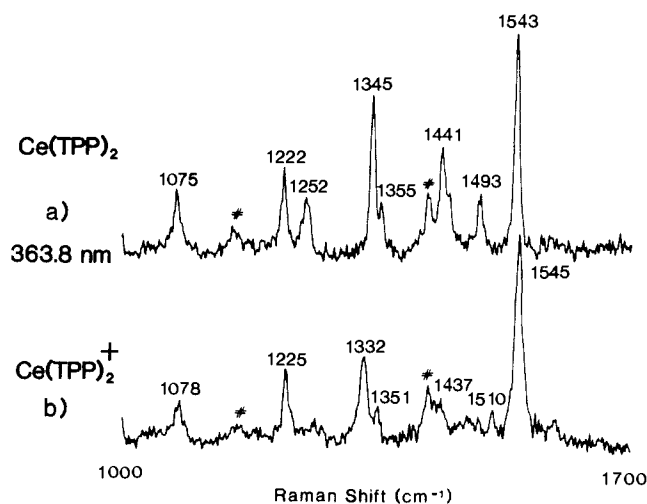
of the neutral and oxidized Ce(IV) OEP and TPP complexes were also obtained with excitation at several other wavelengths in the Soret region (not shown); however, no additional peaks were observed. Because the Ce(OEP)$_2^+$ complex in solution did not yield high quality spectral data, RR spectra were also obtained for solid samples. Insomuch as the frequencies observed for solid and solution samples of the neutral complex are the same (±2 cm^{-1}), we presume that the frequencies for the cation will be similar in the two different media. The vibrational modes which exhibit significant shifts upon oxidation of LuOEPOH and Ce-(OEP)$_2$ are compiled in Table II. The assignments listed in Table II were made on the basis of the observed relative intensities and depolarization ratios and are consistent with those previously made for neutral[50] and cationic[51] OEP complexes.

The general appearance of the RR spectra of both Ce(OEP)$_2^+$ and Ce(TPP)$_2^+$ suggests that the hole is delocalized over the two porphyrin rings of the sandwiches on the RR time scale. In particular, the RR spectra that are observed upon excitation throughout the Soret region (350–450 nm) exhibit a single set of peaks. There is no evidence of composite features due to one neutral and one fully oxidized porphyrin moiety. Such composite RR spectra are typically observed for systems in which the redox orbital is known to be confined to a portion of the molecular framework.[45,52] The relative magnitude of the frequency shifts which occur upon oxidation of LuOEPOH and Ce(OEP)$_2$ provide further evidence for a delocalized ground state (Table II). As can be seen, the oxidation shifts of the modes of the sandwich complex are in all cases less than those of the modes of the monomeric lanthanide porphyrin. Indeed, the shifts observed for the sandwich complex are less than those reported for any monomeric metallo OEP complex.[51] It is noteworthy that the shifts

(48) (a) Norris, J. R.; Uphaus, R. A.; Crespi, H. L.; Katz, J. J. *Proc. Natl. Acad. Sci. U.S.A.* **1971**, *68*, 625–628. (b) Katz, J. J.; Norris, J. R. *Curr. Top. Bioenerget.* **1973**, *5*, 41–75.

(49) Wertz, J. E.; Bolton, J. R. *Electron Spin Resonance*; McGraw-Hill: New York, 1972; pp 336–339.

(50) (a) Kitagawa, T.; Abe, M.; Ogoshi, H. *J. Chem. Phys.* **1978**, *69*, 4516–4525. (b) Abe, M.; Kitagawa, T.; Kyogoku, Y. *Ibid.* **1978**, *69*, 4526–4534.

(51) Oertling, W. A.; Salehi, A.; Chung, Y. C.; Leroi, G. E.; Chang, C. K.; Babcock, G. T. *J. Phys. Chem.* **1987**, *91*, 5887–5898.

(52) Angel, S. M.; DeArmond, M. K.; Donohoe, R. J.; Hanck, K. W.; Wertz, D. W. *J. Am. Chem. Soc.* **1984**, *106*, 3688–3689.
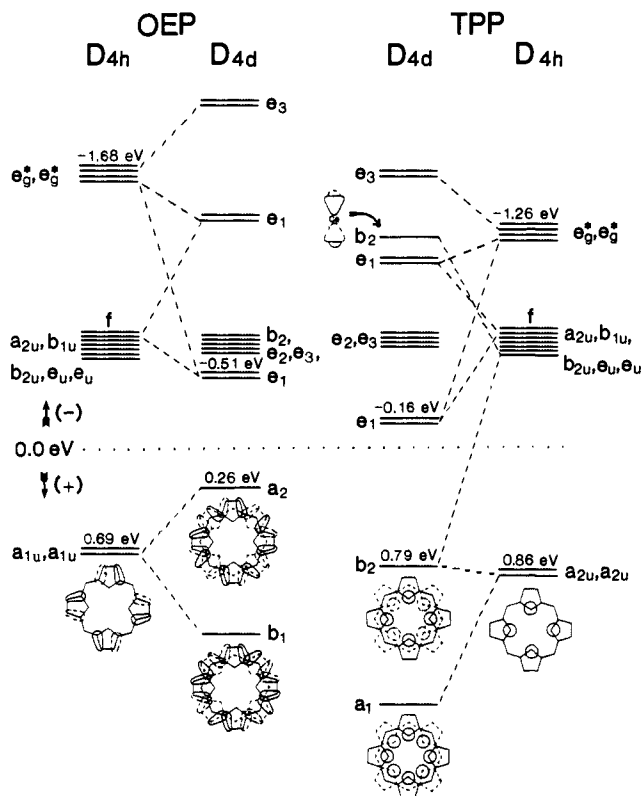
Ce(IV) Porphyrin Sandwich Complexes

J. Am. Chem. Soc., Vol. 110, No. 18, 1988 6123

Figure 7. Orbital energy diagram for the Ce(IV) porphyrin sandwich complexes examined in this study (see text).

of the ν_2, ν_4, and ν_{11} modes of Ce(OEP)$_2$ are approximately $^1/_2$–$^2/_3$ of those of LuOEP.OH. A reduction in the magnitudes of the oxidation shifts is expected if the redox orbital is delocalized over both porphyrin π systems because only $^1/_2$ an electron is effectively removed from each ring. [It should be noted that the different magnitude of the oxidation shifts of LuOEPOH versus Ce(OEP)$_2$ cannot be due to differential changes in structure which occur upon oxidation. Oertling et al.[51] have shown that the magnitude of the oxidation shifts of the skeletal modes (with the exception of ν_4) of metallo OEP complexes are essentially independent of structural features such as core size and extent of doming.]

IV. Discussion

The spectroscopic data presented above indicate that the holes in both Ce(OEP)$_2{}^+$ and Ce(TPP)$_2{}^+$ are delocalized on the time scale of vibrational motion (10^{-13} s) and probably on the time scale of electronic motion (10^{-15} s). In the case of Ce(OEP)$_2{}^+$, the redox orbital does not contain substantial metal character which suggests that delocalization occurs as a result of direct porphyrin–porphyrin interaction. On the other hand, the redox orbital of Ce(TPP)$_2{}^+$ clearly contains a non-negligible metal contribution; thus, delocalization in this system may be facilitated by participation of the metal ion. These results can be rationalized by inspection of the molecular orbitals of the OEP and TPP complexes as well as the f orbitals of the Ce(IV) ion. A partial molecular orbital diagram for these systems is shown in Figure 7. In the left-most and right-most portions of the figure, the porphyrin and metal orbitals, labeled according to D_{4h} symmetry, are shown in the limit of zero porphyrin–porphyrin and metal–porphyrin interaction. In the central portion of the figure, the various orbitals are shown in the limit of strong porphyrin–porphyrin interaction. These orbitals are labeled according to D_{4d} symmetry which is the actual symmetry of Ce(OEP)$_2{}^{31d}$ and the presumed symmetry of Ce(TPP)$_2$. The relative energies and extent of metal–porphyrin interaction indicated in the figure are in accord with the electrochemical and spectroscopic results and will be discussed further below.

The highest occupied molecular orbitals (HOMO) of the OEP and TPP sandwich complexes are derived from a_{1u} and a_{2u} monomer orbitals, respectively. The former orbital contains electron

density primarily at the C_α and C_β carbon atoms of the pyrrole rings, whereas the latter contains density primarily at the pyrrole nitrogen and methine bridge carbon atoms.[53] Although the 45° interring torsional angle of the D_{4d} structure staggers the nitrogen atoms on opposite porphyrin rings, these atoms are still in close proximity (~ 3 Å). In addition, the C_α pyrrole atoms on opposite macrocycles are approximately eclipsed and still within van der Waals contact (~ 3.2 Å).[31d] On the basis of these spatial characteristics, the interactions between the a_{2u} orbitals on the two halves of the sandwich would be expected to be greater than those between the a_{1u} orbitals. Strong interactions between the monomer a_{1u} and a_{2u} orbitals would result in bonding and antibonding pairs as is depicted in Figure 7. Only the pairs derived from the pertinent monomeric redox orbitals are shown in the figure (for clarity, only the interacting lobes of the π orbitals are shown). Under D_{4d} symmetry, the metal f orbitals transform as b_2, e_1, e_2, and e_3. Thus, there are no metal f orbitals of appropriate symmetry to mix with the HOMO of Ce(OEP)$_2$. On the other hand, the b_2 metal- and porphyrin-centered orbitals can mix to form the HOMO of Ce(TPP)$_2$. Unlike the HOMOs, the lowest unoccupied molecular orbitals (LUMO) of Ce(OEP)$_2$ and Ce(TPP)$_2$ are primarily metal-centered. These LUMOs may contain some porphyrin character due to the symmetry equivalence of the metal and porphyrin e_1 orbitals. The latter are derived from bonding interaction between the monomeric porphyrin $e_g{}^*$ orbitals. In the construction of the molecular orbital diagram, the potentials for the first oxidation and first reduction of the closed shell (f^{14}) Lu(III) complexes were used to establish approximate energies for the orbitals of OEP and TPP. This seems justified because these potentials are typical of those observed for other closed shell metalloporphyrins.[41] The energies of the HOMOs and LUMOs of the two sandwich porphyrin complexes were then placed on the diagram according to the observed electrochemical potentials. The empty f orbitals of the Ce(IV) ion were assumed to lie at the same energy in the OEP and TPP complexes prior to mixing with the porphyrin orbitals.

The molecular orbital description for Ce(OEP)$_2{}^+$ is less complicated than that for Ce(TPP)$_2{}^+$ because oxidation involves an orbital that is purely porphyrin in character. Accordingly, the oxidation potential of Ce(OEP)$_2$ relative to that of LuOEPOH should yield an approximate measure of the porphyrin–porphyrin interaction energy in the sandwich complex. The Ce(OEP)$_2$ species is 0.43 V easier to oxidize than the Lu(III) monomer. This energy is nominally one half the splitting between the bonding (b_1) and antibonding (a_2) pair derived from the a_{1u} monomer orbitals. In this picture, promotion of an electron from the b_1 to the a_2 orbital represents a z-polarized, allowed electronic transition. It is especially noteworthy that the predicted energy for this transition (0.86 eV) is quite close to that observed for the near IR transition of Ce(OEP)$_2{}^+$ (0.96 eV).[31c] This band has previously been assigned as an intervalence charge-transfer transition; however, in that the spectroscopic data presented herein indicate that the ground state of the cation is delocalized, this description is not accurate. Given the similarity between the predicted splitting of the bonding and antibonding HOMO pair and the observed energy of the near IR transition, it seems likely that this band is due to a transition between the two delocalized molecular orbitals.

The molecular orbital description for Ce(TPP)$_2{}^+$ is more complicated than that for Ce(OEP)$_2{}^+$ because the redox orbital contains metal character. This metal participation precludes a direct assessment of the porphyrin–porphyrin interaction energy on the basis of the oxidation potential of Ce(TPP)$_2$ relative to that of LuTPPOH. As was previously noted, the interaction between the a_{2u} macrocycle orbitals is expected to be greater than that between the a_{1u} orbitals. Thus, the difference in the oxidation potential of Ce(TPP)$_2$ relative to LuTPPOH should be greater than that of Ce(OEP)$_2$ relative to LuOEPOH (in the absence of metal involvement in the redox orbital). In addition, the near IR

(53) Gouterman, M. In *The Porphyrins*; Dolphin, D., Ed.; Academic Press: New York, 1978; Vol. III, pp 1–165.

transition of Ce(TPP)$_2^+$ should be at higher energy than that of Ce(OEP)$_2^+$. In fact, the first oxidation potential of Ce(TPP)$_2$ is similar to that of LuTPPOH, and the near IR transition of Ce(TPP)$_2^+$ is at an energy (0.92 eV) which is slightly less than that of Ce(OEP)$_2^+$.[31c] Both of these results reflect mixing of metal f orbital character into the HOMO as is shown in Figure 7. Such mixing results in a ground-state wave function which contains partial metal f^1/porphyrin dication character. The inclusion of Ce(III) character in the wave function is probably the cause of the significant anisotropy and rapid relaxation observed in the EPR spectrum of Ce(TPP)$_2^+$. The occurrence of significant mixing of the metal f and porphyrin π orbitals is supported by quasirelativistic SCF-Xα scattered-wave calculations on cerocene complexes.[54] These calculations indicate that the f orbitals of the Ce(IV) ion are capable of an unusually large degree of covalent interaction with ligand orbitals. It should be noted that this type of orbital mixing is not expected for f^{14} Lu(III) complexes. The ^{175}Lu hyperfine interactions manifested in the isotropic EPR spectrum of (LuTPPOH)$^+$ are due to spin polarization effects.

The mixing of the metal and porphyrin orbitals is also manifested in the potentials for the first reductions of the two sandwich complexes. For both the OEP and TPP systems, the e$_1$ bonding orbitals (derived from the e$_g$* monomer orbitals) are capable of mixing with the metal f orbitals. The reduction potential observed for Ce(TPP)$_2$ versus Ce(OEP)$_2$ indicates that this mixing is greater in the former complex than in the latter as is schematically represented in Figure 7. This more extensive mixing in the TPP sandwich probably occurs because the metal and porphyrin e$_1$ orbitals of this complex are energetically closer than those of the

OEP sandwich. The relative ease of reduction of LuTPPOH (-1.26 V) versus LuOEPOH (-1.68 V) lends credence to this conclusion.

V. Conclusions

The hole delocalization which is observed for the two oxidized Ce(IV) sandwich porphyrins occurs primarily as a result of the close proximity of the macrocycles. The exact mechanism for delocalization (orbital overlap, strong exciton, etc.) is not immediately obvious and will require detailed theoretical studies. Regardless, hole delocalization in the dimeric systems has interesting implications for higher order aggregates. It might be speculated that if stacked aggregates of the form Ce$_n$(porphyrin)$_{n+1}$(L$^-$)$_{an}$ could be synthesized, these systems would be highly conducting (L$^-$ is a counterion for charge conservation). To date, such high order aggregates have not been prepared; however, the triple-decker Ce(III) sandwich, Ce$_2$(OEP)$_3$, is known.[31a,b,d] This suggests that higher order oligomers may be obtainable. The stacked lanthanide porphyrin systems may offer certain advantages over stacked metallophthalocyanines in that a$_{2u}$-like orbitals are available for oxidation in the former systems but not the latter.[10,13,53] Involvement of these orbitals in hole delocalization facilitates participation of the metal ion and may enhance conductivity. The assessment of conductivity in lanthanide porphyrin polymers must, however, await their synthesis.

(54) Rösch, N.; Streitwieser, A., Jr. J. Am. Chem. Soc. 1983, 105, 7237-7240.

Mechanistic Studies of Alkene Epoxidation Catalyzed by Nickel(II) Cyclam Complexes. ^{18}O Labeling and Substituent Effects

Joanne F. Kinneary, Jeffrey S. Albert, and Cynthia J. Burrows*

Contribution from the Department of Chemistry, State University of New York at Stony Brook, Stony Brook, New York 11794-3400. Received January 4, 1988

Abstract: The oxidations of cyclohexene and various aryl-substituted alkenes are catalyzed by the cyclam (1,4,8,11-tetraazacyclotetradecane) complex of Ni(NO$_3$)$_2$ with iodosylbenzene as terminal oxidant. Epoxides are the major products; however, small amounts of ring-opened products, over-oxidation to ketones or aldehydes, and allylic oxidation of cyclohexene are also observed. *E* olefins are more reactive than the corresponding *Z* olefins in contrast to the results of iron porphyrin catalysis, and kinetic studies of para-substituted styrenes indicate that the reaction is facilitated by electron-donating substituents. Labeling studies with PhI^{18}O confirm that the epoxide oxygen is derived from PhIO while allylic oxidation and over-oxidation products involve both PhIO and exogenous sources of oxygen. A pericyclic mechanism for the formation of PhCHO is proposed along with the intermediacy of a high-valent nickel–oxo complex as the active oxidant. These results are discussed in light of related transition-metal/PhIO oxidation mechanisms.

The mechanisms by which transition-metal complexes mediate olefin oxidation have intrigued organic, inorganic, and biological chemists alike.[1] In organic synthesis, an understanding of the mechanistic features critical to high stereoselectivity is desired for the design of new oxidation catalysts. In the biological realm,

monooxygenase enzymes, including cytochrome P-450 and various peroxidases, employ iron(III) porphyrins at their active sites in order to effect oxygen atom transfer to olefins and other substrates. Their mechanisms and those of numerous model systems have been the subject of considerable discussion.[2,3] Most of these studies

(1) (a) Sheldon, R. A.; Kochi, J. K. Metal-Catalyzed Oxidations of Organic Compounds; Academic: New York, 1981. (b) Holm, R. H. Chem. Rev. 1987, 87, 1401-1449.

(2) Ortiz de Montellano, P. R., Ed. Cytochrome P-450: Structure, Mechanism, and Biochemistry; Plenum: New York, 1976.

(3) Guengerich, F. P.; Macdonald, T. L. Acc. Chem. Res. 1984, 17, 9-16.